Mon. Not. R. Astron. Soc. **380,** 839–847 (2007) doi:10.1111/j.1365-2966.2007.12147.x

High-precision wavelength calibration of astronomical spectrographs with laser frequency combs

M. T. Murphy,[1⋆] Th. Udem,[2] R. Holzwarth,[2] A. Sizmann,[2] L. Pasquini,[3] C. Araujo-Hauck,[3] H. Dekker,[3] S. D'Odorico,[3] M. Fischer,[2] T. W. Hänsch[2] and A. Manescau[3]

[1]*Institute of Astronomy, University of Cambridge, Madingley Road, Cambridge CB3 0HA*
[2]*Max-Planck Institut für Quantenoptik, Hans-Kopfermann-Strasse 1, 85748 Garching, Germany*
[3]*European Southern Observatory, Karl-Schwarzschild-Str. 2, 85748 Garching, Germany*

Accepted 2007 June 18. Received 2007 June 12; in original form 2007 March 16

ABSTRACT

We describe a possible new technique for precise wavelength calibration of high-resolution astronomical spectrographs using femtosecond-pulsed mode-locked lasers controlled by stable oscillators such as atomic clocks. Such 'frequency combs' provide a series of narrow modes which are uniformly spaced according to the laser's pulse repetition rate and whose absolute frequencies are known a priori with relative precision better than 10^{-12}. Simulations of frequency comb spectra show that the photon-limited wavelength calibration precision achievable with existing echelle spectrographs should be $\sim$1 cm s^{-1} when integrated over a 4000 Å range. Moreover, comb spectra may be used to accurately characterize distortions of the wavelength scale introduced by the spectrograph and detector system. The simulations show that frequency combs with pulse repetition rates of 5–30 GHz are required, given the typical resolving power of existing and possible future echelle spectrographs. Achieving such high repetition rates, together with the desire to produce all comb modes with uniform intensity over the entire optical range, represents the only significant challenges in the design of a practical system. Frequency comb systems may remove wavelength calibration uncertainties from all practical spectroscopic experiments, even those combining data from different telescopes over many decades.

Key words: instrumentation: detectors – instrumentation: spectrographs – methods: laboratory – techniques: spectroscopic.

1 INTRODUCTION

Echelle spectrographs are the basic tool for astronomical spectroscopy with high velocity precision. Since many echelle diffraction orders can be cross-dispersed and thereby recorded simultaneously on rectangular-format media [e.g. modern charge-coupled devices (CCDs)], more-or-less continuous wavelength coverage over much of the optical range can be achieved whilst maintaining high resolving power.[1] Most modern echelle spectrographs operate at $R = 30\,000-150\,000$; higher resolving powers usually entail reduced wavelength coverage. However, to fully exploit the velocity precision available in high-resolution spectra, precise wavelength calibration over much of the available wavelength range is usually required. For example, searches for extra-solar planets via the radial velocity method (e.g. Mayor & Queloz 1995; Marcy & Butler 1996) have achieved night-to-night relative precisions better than 1 m s^{-1} from stellar absorption lines integrated over wavelength ranges of $\sim$1000 to 3000 Å (e.g. Rupprecht et al. 2004; Lovis et al. 2006). Also, echelle spectra of quasar absorption systems have constrained cosmological variations in fundamental constants, such as the fine-structure constant (e.g. Bahcall, Sargent & Schmidt 1967; Webb et al. 1999) and proton-to-electron mass ratio (e.g. Varshalovich & Levshakov 1993; Ivanchik et al. 2005). Recent measurements of α-variation using many absorption systems reach relative precisions of $\sim 10^{-6}$ when comparing several transitions separated by up to $\sim$5000 Å (e.g. Murphy et al. 2001; Murphy, Webb & Flambaum 2003). The corresponding velocity precision required is $\sim$20 m s^{-1}.

The need for even higher precision is already clear. Detecting Earth-mass extra-solar planets around solar-mass stars will require $\lesssim$10 cm s^{-1} precision stable over many-year time-scales. Also, current evidence for varying constants (e.g. Murphy et al. 2004;

⋆E-mail: mim@ast.cam.ac.uk (MTM)

[1] Resolving power $R \equiv \lambda/\mathrm{FWHM}$, where FWHM is the instrumental profile's (IP) full width at half-maximum.

Table 1. The requirements for an ideal wavelength calibration source and the relative advantages and disadvantages of three current sources plus the frequency comb possibility we describe in this paper. We consider a spectrograph with resolving power $R \sim 150\,000$. 'Poss.' means possible depending on the design and construction of the calibration source.

Calibration lines	ThAr	I_2 cell	Etalon	Comb
From fundamental physics	Yes	Yes	No	Yes
Individually unresolved	Mostly	Yes	Poss.	Yes
Resolved from each other	No	No	Poss.	Poss.
Uniformly spaced	No	No	Yes	Yes
Cover optical range	Yes	No	No	Poss.
Uniform strength	No	No	Poss.	Poss.
Long-term stability	No	Poss.	No	Yes
Maintain object S/N	Yes	No	Yes	Yes
Exchangeable	Yes	Yes	Poss.	Yes
Easy to use	Yes	Yes	Poss.	Poss.
Reasonably low cost	Yes	Yes	Yes	Poss.

Reinhold et al. 2006) remains controversial and such potentially fundamental results should be refuted or confirmed with the highest possible confidence. There is even the possibility of measuring the acceleration of the Universal expansion by monitoring the change in redshift of Lyman α forest absorption lines in quasar spectra (e.g. Sandage 1962; Loeb 1998). This would require two epochs of spectra, taken decades apart, with velocity precision approaching 1 cm s^{-1} integrated over $\sim$1000$-$3000 Å ranges. This is one possible aim of the Cosmic Dynamics Experiment (CODEX) spectrograph proposed for the European Extremely Large Telescope (Pasquini et al. 2006; Grazian et al. 2007; Liske et al., in preparation).

Astronomical echelle spectra are usually wavelength calibrated using comparison emission- or absorption-line spectra. The ideal comparison spectrum would comprise a series of lines which (i) have known wavelengths which are determined by fundamental physics; (ii) are individually unresolved; (iii) are resolved from each other; (iv) have uniform spacing; (v) cover the entire optical wavelength range; (vi) have uniform strength (intensity or optical depth); (vii) are stable over long time-scales and (viii) do not reduce the signal-to-noise ratio (S/N) of the object spectrum. The calibration source should also be (ix) exchangeable, in the sense that two independent sources produce the same spectrum; (x) easy to use, i.e. essentially 'turn-key' operation for non-expert users and (xi) should have a reasonably low cost. Table 1 summarizes whether four different calibration sources meet these requirements. The most commonly used calibration source is the thorium–argon (ThAr) hollow-cathode emission-line lamp. While it is of relatively low cost, has lines whose wavelengths are determined by atomic physics and which cover the entire optical wavelength range, it has several disadvantages. For example, ThAr lines differ widely in intensity and spacing. Indeed, most are blended together at $R \lesssim 150\,000$. Furthermore, as the current and pressure in the lamp vary (e.g. as the lamp ages) the relative intensity of different ThAr lines varies widely. Iodine cells are also commonly used in radial-velocity extra-solar planet searches (e.g. Marcy & Butler 1992). These have similar advantages and disadvantages as ThAr lamps but they are typically only useful over the wavelength range 5000–6500 Å and absorb about half the object light, thereby significantly reducing the S/N.

A significant step towards the ideal calibration source might be achieved with the relatively new technology of optical 'frequency combs' generated from mode-locked femtosecond-pulsed lasers. The 2005 Nobel Prize in physics was awarded for the pioneering work on such combs (e.g. Reichert et al. 1999; Jones et al. 2000; Udem, Holzwarth & Hänsch 2002). As the name suggests, a frequency comb provides a spectrum of continuous-wave laser lines called modes. They are produced by the repetitive pulse train of the mode-locked laser. The mode spacing, which is constant in frequency space, is given by the pulse repetition frequency. Since it resides in the radio frequency domain, it can readily be synchronized with an extremely precise frequency reference such as an atomic clock. The comb's perfectly regular frequency grid should also facilitate the effective compensation of non-linearities in the spectrograph's calibration curve while directly linking the calibration to the fundamental physics of the atomic clock. This direct link to the definition of time and the long-term stability means that even if different combs are used to calibrate spectra taken at (perhaps widely) different epochs, those spectra can be directly compared. Research utilizing archival and 'virtual observatory' data would directly benefit from such a reproducible calibration source. These properties would greatly facilitate extra-solar planet detection and varying-constant analyses and would be more-or-less required for detecting the Universal acceleration via Lyman α forest spectra taken decades apart.

This paper further describes the possibility of frequency comb calibration of echelle spectrographs. Section 2 outlines the basics of frequency comb generation, the methods used to ensure that they are stable and the general manner in which they might be used as practical echelle calibration sources. Section 3 derives the optimal laser repetition frequency and the overall precision of the wavelength calibration that might be achieved with typical echelle spectrographs. Some likely sources of systematic errors which may otherwise limit the precision are also discussed. Section 4 outlines the main challenges in designing a working frequency comb calibration system and proposes some possible solutions.

2 BASIC OPERATION

2.1 Generating the comb

The exact properties of a frequency comb may be derived even without the knowledge of the operational principles of a mode-locked laser. It suffices to know that these lasers can store a single pulse and maintain it on a repetitive path. After each round trip, a copy of this pulse is emitted though the output mirror/coupler of the laser, resulting in an indefinite train of laser pulses. Like in any other laser, the energy lost is replenished by stimulated emission in the lasing medium, thereby allowing the energy in a short pulse to be stored for any length of time by compensation of loss with gain.

To understand the mode structure of a femtosecond frequency comb and the techniques employed to stabilize it, consider the idealized case of a pulse circulating as a carrier wave with frequency ν_c in a laser cavity with length L. The cavity strongly modulates the carrier wave amplitude which can therefore be described by a periodic envelope function $A(t) = A(t - T)$, where T is the round trip travel time of the pulse calculated from the cavity mean group velocity: $T = 2L/v_{gr}$. The repetition rate of the laser is simply $\nu_r = 1/T$. This is illustrated in Fig. 1. Since the envelope function is periodic, it can be written as a Fourier series and the electric field at any given place (e.g. the laser's output mirror/coupler) can therefore be written as

$$E(t) = A(t)e^{-i\,2\pi\nu_c t} = \sum_m A_m e^{-i\,2\pi(m\nu_r+\nu_c)\,t}, \quad (1)$$

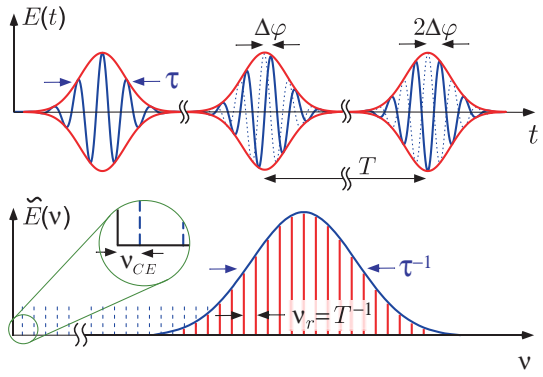

Figure 1. A pulse train (top) produces the optical frequency comb in Fourier space (bottom) with some properties inverted. Shorter pulse envelopes produce broader frequency combs. The round trip time of the pulses inside the generating laser cavity (not shown) determines the repetition frequency, ν_r, exactly. Dispersive elements in the laser cause a difference in the group and phase velocity, continuously shifting the carrier wave with respect to the envelope in the upper trace by $\Delta\varphi$ per pulse. In the frequency domain, this causes the comb to shift by an amount $\nu_{ce} = \Delta\varphi/2\pi T$.

where A_m is the mth Fourier component of $A(t)$. Equation (1) shows that, under the assumption of a periodic pulse envelope, the resulting spectrum is a comb of laser frequencies with spacing ν_r such that the mth frequency component is $\nu_m = m\nu_r + \nu_c$. In general, ν_c is not an integer multiple of ν_r and so the modes are shifted from being exact harmonics of ν_r. Renumbering the modes gives

$$\nu_n = n\nu_r + \nu_{ce} \tag{2}$$

for n a large integer, where the carrier envelope offset frequency, ν_{ce}, is restricted to $0 \leqslant \nu_{ce} < \nu_r$. This equation maps two radio frequencies, ν_r and ν_{ce} – which can be stabilized by a precise reference such as an atomic clock – on to the optical frequencies ν_n.

Given the simple treatment above, one might expect deviations from equation (2) in reality. However, mode locking the laser ensures that equation (2) is realized to very high precision in practice. The frequencies ν_n in equation (2) represent the longitudinal cavity modes of the mode-locked laser. The process of mode locking stabilizes the mode frequency difference, ν_r, and the cavity mode phases such that their superposition yields a short pulse. The existence of such a pulse depends on the stability of the relative phases of the modes: if these change in time – for example, due to a small deviation of the mutual mode separation from ν_r – the pulse would disintegrate immediately. The very observation that the pulse stays intact for a time Δt implies that variations in ν_r must be $<1/\Delta t$. For a pulse lifetime of 1 s, this is only a few parts in 10^{14} at the optical frequencies ν_n. Of course, the stored pulse lasts much longer than 1 s. In fact, deviations from equation (2) – that is, deviations from a constant mode spacing – have so far evaded detection even at the $\sim 10^{-16}$ level (Holzwarth et al. 2000).

As the pulse circulates in the cavity, dispersion causes a difference between the group and phase velocities. The pulse envelope, $A(t)$, propagates at the group velocity, v_{gr}, while the carrier wave travels at its phase velocity, causing them to shift with respect to each other after each pulse round trip. This is illustrated in Fig. 1. Comparing two consecutive pulses with $A(t) = A(t - T)$, equation (1) implies that the electric field is given by

$$E(t) = E(t - T)\mathrm{e}^{-i\,2\pi\nu_c T} = E(t - T)\mathrm{e}^{-i\,2\pi\nu_{ce} T} \tag{3}$$

where, in the last step, a large integer multiple of $2\,\pi$ was subtracted from the phase, equation (2) was used with ν_c as one of the modes and we recall that $\nu_r = T^{-1}$. That is, the phase shift for each pulse round trip is $\Delta\varphi = 2\pi\,\nu_{ce} T$. Therefore, the frequency comb is offset from being exact integer harmonics of ν_r by the so-called carrier-envelope offset frequency, $\nu_{ce} = \Delta\varphi/2\pi T$ (Udem et al. 2002). It should be emphasized that the *model* for the origin of ν_{ce} is not important for precision measurements using the comb; all that is required is that ν_{ce} can be fixed to a certain value experimentally (e.g. via a feedback loop) and that the mode spacing, ν_r, is constant.

As Fig. 1 illustrates, the spectral envelope of the frequency comb has a width that is *roughly* given by the inverse of the pulse duration and a mode spacing given *exactly* by the inverse round trip time, $\nu_r = T^{-1}$. Modern mode-locked lasers readily achieve $\sim$100 THz wide spectra ($\approx$830 Å wide at 5000 Å) from $\sim$10 fs pulses. Two types of lasers are common: the titanium–sapphire Kerr-lens mode-locked laser which operates around 8000 Å and the erbium- and ytterbium-doped fibre lasers which operate at around 1.55 and 1.04 μm, respectively. Typical values for the mode spacing/repetition frequency are $\nu_r \sim 100$ MHz, but in some special cases up to $\nu_r \sim 40-160$ GHz has been achieved (see further discussion in Section 4).

2.2 Self-referencing the comb

Measuring and/or stabilizing both radio frequencies, ν_{ce} and ν_r, fix the entire optical frequency comb by virtue of equation (2). While the pulse repetition rate, ν_r, is readily measured with a photodetector somewhere in the beam, the determination of ν_{ce} requires significant effort. In fact, it took more than 20 yr to develop a simple ν_{ce} detection scheme, dubbed 'self-referencing', which is illustrated in

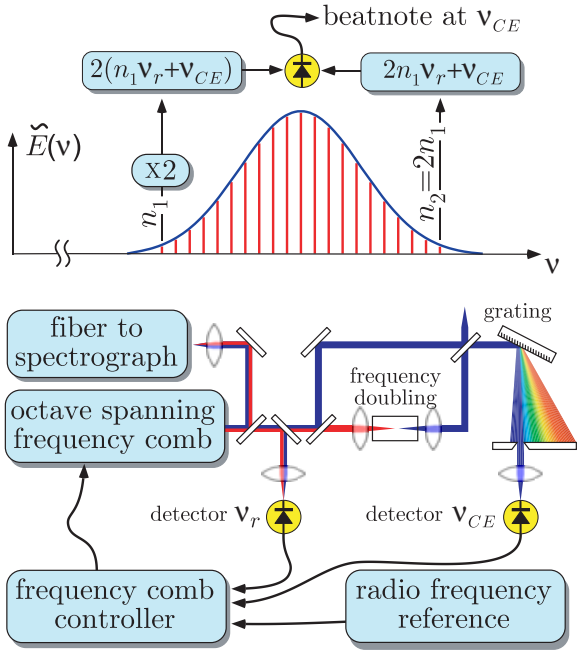

Figure 2. A typical self-referencing scheme. Top: the carrier envelope offset frequency, ν_{ce}, that displaces the modes from being exact harmonics of the repetition rate, ν_r, is measured by frequency doubling some modes at the 'red' side of the comb and beating them against modes at the 'blue' side (depending on the type of laser, these do not need to be truly blue or red). Bottom: such a self-referencing scheme employs a dichroic mirror to separate the 'red' and 'blue' wings of the frequency comb. The former is frequency doubled in a non-linear crystal and reunited with the 'blue' part to create a wealth of beat frequencies, all at ν_{ce}.

Fig. 2. A low-frequency mode with mode number n_1 is frequency doubled to frequency $2(n_1\nu_r + \nu_{ce})$. This is superimposed with a high-frequency mode, n_2, on to a photodetector. The resulting beat frequency is therefore $(2n_1 - n_2)\nu_r + \nu_{ce}$ which reduces to the desired signal, ν_{ce}, provided that $2n_1 = n_2$. This latter condition requires the comb to span an entire optical octave. Lasers capable of producing such broad spectra are only now becoming available (e.g. Matos et al. 2004; Fortier, Bartels & Diddams 2006); they are currently experimental and have several disadvantages. The standard method of producing this spectral width has therefore been via a process called self-phase modulation induced by non-linear interactions in optical fibres.[2] For practical pulse repetition rates in the radio frequency domain, especially those approaching the GHz regime, the required peak intensity for such non-linear processes is difficult to achieve because the available laser power is shared by more pulses. However, with the development of Kerr-lens mode-locked lasers and photonic crystal fibres (e.g. Knight et al. 1996), octave-spanning combs can now be simply generated. The fibre lasers mentioned above use specially doped fibres to achieve similar spectral broadening.

Self-referencing applies the full accuracy of the radio frequency reference to the entire optical comb, yielding a perfectly regular calibration grid for the spectrograph. Current commercial caesium atomic clocks would provide a calibration as precise as several parts in 10^{13}, i.e. a velocity precision of $\sim$0.01 cm s^{-1}. This may even be improved by using a timing signal broadcasted by the Global Positioning System to further stabilize the caesium clock or by setting up a local caesium fountain clock (e.g. Bauch 2003). However, in Section 3 we demonstrate that typical echelle spectrographs will limit the available precision to $\sim$1 cm s^{-1} and so such improvements should not be necessary.

In contrast to this standard radio-frequency self-referencing, an alternative optical referencing scheme might prove more practical for astronomical applications. In such a scheme, the nth optical mode, ν_n, could be stabilized, for example, to an iodine-stabilized laser. The repetition rate would be stabilized to a precise radio frequency reference just as in the standard scheme above. As iodine-stabilized lasers can be as accurate as a few parts in 10^{13} (e.g. Ye, Ma & Hall 2001) this method could also provide the required accuracy.

2.3 The comb as a calibration source

Fig. 2 shows the self-referenced (i.e. frequency-calibrated) comb spectrum being fed into the echelle spectrograph via an optical fibre. We envisage that such a configuration would offer the greatest stability and potential for tracking real-time distortions of the spectrograph wavelength scale. In practice, the spectrograph would be fed by two fibres, one carrying the science object light and the other carrying the comb light for calibration. The two spectra would be recorded simultaneously next to each other on the CCD. The intensity of the frequency comb spectrum might be varied according to changes in the intensity of object light being transmitted by the telescope and spectrograph. Such variations could easily be tracked via feedback from detection of stray object light as the main beam passes into the spectrograph. Thus, changes in the weather conditions or small drifts in the spectrograph itself during the object exposure, which might ordinarily lead to distortions of the wavelength scale, would affect the recorded comb spectrum in the same way.

Of course, for very high-precision work, one would have to consider other instrumental effects, such as differences between (and inhomogeneities in) the object and comb beam profiles as they emerge from the fibres. One would also consider placing the entire spectrograph in vacuum to ensure temperature and pressure stability. Many of the above techniques have already been demonstrated (e.g. Baranne et al. 1996; Mayor et al. 2003). Of course, the more traditional approach of taking calibration exposures before and/or after the object exposure would still be open with the comb as a calibration source. The comb light could also be expanded and diffused after emerging from the fibre to illuminate a traditional spectrograph slit.

Note that the specifics of a final frequency comb design and spectrograph feed system need careful consideration quite beyond the scope of this paper. Indeed, these design considerations first require knowledge of the optimal laser repetition rate for typical echelle resolutions. The various tolerances involved in the design should also be informed by the photon-limited calibration precision achievable with an echelle spectrograph. These quantities are calculated in Section 3 and their implications for design challenges are considered in Section 4.

3 OPTIMAL PHOTON-LIMITED WAVELENGTH CALIBRATION PRECISION

The wavelength calibration precision available from a comb spectrum will clearly improve with increasing line density. However, since the spectrograph resolving power is finite, too high a line density will decrease the contrast between neighbouring lines and degrade the available precision; an optimal line spacing must exist. Here, we calculate this optimum laser repetition rate and the associated wavelength calibration precision. We first present a simple estimate of the photon-limited precision using some general arguments in Section 3.1. Sections 3.2 and 3.3 describe more rigorous calculations which also provide the optimal laser repetition rate. These calculations concentrate only on the photon-limited precision and ignore systematic errors; the latter are discussed briefly in Section 3.4. We assume throughout this section that only one CCD exposure of the comb spectrum is used for wavelength calibrating the spectrograph. The dynamic range of the CCD pixels therefore limits the comb S/N. Clearly, future improvements in detector technology, such as multiple or continuous reading out of the comb spectrum during a single science exposure, could improve the effective comb S/N, thereby allowing even more precise calibration.

3.1 General considerations

Some general arguments serve as an intuitive introduction to the calculations in the following sections. Let us first consider a single unresolved comb line. When extracted from the CCD, this line will reflect the IP of the spectrograph. Assuming this to be a Gaussian whose FWHM is sampled by $n > 1$ pixels, a well-known approximation to the error on the line's position is (e.g. Brault 1987)

$$\delta v \approx A \frac{\mathrm{FWHM}}{\mathrm{S/N} \times \sqrt{n}}. \quad (4)$$

[2] Self-phase modulation originates from an intensity-dependent refractive index of the material. In particular, the polarizability of the material behaves non-linearly with respect to the incident electromagnetic field. This is also called the 'Kerr effect'. It provides an additional phase delay proportional to the field's intensity distribution (in both space and time). Applications in the context of the calibration comb include intensity-dependent lensing for mode locking ('Kerr-lens mode-locking') in femtosecond lasers and spectral broadening or ultrafast pulse shaping.

The S/N here refers to the peak S/N per pixel across the line (i.e. usually at the line centre). The pre-factor, A, depends on both the functional form of the line profile and the relationship between S/N and pixel intensity. For example, if the noise level is constant across the profile then $A = 0.693$ for a Gaussian and 0.798 for a Lorentzian (Brault 1987). In our case, the noise is Poissonian with an additional small contribution from detector noise. From a simple numerical experiment in which Gaussian profiles with this noise profile were fitted with standard least-squares techniques, we find that $A \approx 0.41$ when the photon noise dominates the detector noise.

To determine the total velocity precision available from, say, an entire echelle order containing such comb lines, we must know the line density and the spectral width of the order. As a first guess, let us assume that a comb line occurs every 2.5 resolution elements so that the line density is high but neighbouring lines do not strongly overlap. For consistency with the more rigorous calculations below, let us assume that echelle orders are 2048 pixels long with three-pixel sampling of the FWHM. That is, there are $N \approx 272$ comb lines per echelle order. Therefore, assuming a peak S/N = 500 in each line, the total calibration precision per echelle order at $R = 150\,000$ (i.e. FWHM = 2 km s^{-1}) is $\sigma_{\rm v} \approx \delta v/\sqrt{N} = 0.41 \times 2\,{\rm km\,s^{-1}}/(500 \times \sqrt{3 \times 272}) = 5.7\,{\rm cm\,s^{-1}}$.

The following sections demonstrate that our assumption that comb lines should be spaced by ∼2.5 resolution elements does in fact provide an optimal calibration with precision close to 6 cm s^{-1} per echelle order as predicted above.

3.2 Velocity information content of comb spectra

If a small[3] velocity change is to be measured from pixel i in a spectrum $F(i)$ with 1σ error array $\sigma_F(i)$, the limiting velocity precision is given by (Bouchy, Pepe & Queloz 2001)

$$\frac{\sigma_{\rm v}(i)}{c} = \frac{\sigma_F(i)}{\lambda(i)\,[\partial F(i)/\partial\lambda(i)]}. \tag{5}$$

This equation simply states that a more precise velocity measurement is available from those pixels where the flux has a large gradient and/or the uncertainty in the flux is small. We have used wavelength as the dispersion coordinate here but one may replace λ with any other dispersion measure desired, including pixels. This quantity can be used as an optimal weight,

$$W(i) = [\sigma_{\rm v}(i)/c]^{-2}, \tag{6}$$

to derive the total velocity precision available from all pixels in a spectrum,

$$\frac{\sigma_{\rm v}}{c} = \frac{1}{\sqrt{\sum_i W(i)}}. \tag{7}$$

If the spectrum is divided into smaller spectral slices k, such as echelle orders, then it follows that the total velocity precision available is a weighted average of that available from each slice,

$$\sigma_{\rm v} = \frac{1}{\sqrt{\sum_k \sigma_{\rm v}^{-2}(k)}}. \tag{8}$$

[3] In all applications discussed in this paper, the expected velocity change is much smaller than the width of any spectral feature.

3.3 Simulations of comb echelle spectra

Equations (7) and (8) can be used to calculate the velocity precision achievable with a frequency comb recorded with an echelle spectrograph. To this end, we construct a simple model of a frequency comb spectrum by writing the flux in each pixel, measured in photoelectrons, as the product of a slowly varying 'envelope function' $F_{\rm e}(i)$ and a quickly varying 'comb function' $f(i)$ which varies between zero and unity: $F(i) = f(i)F_{\rm e}(i)$. A reasonable model of the expected 1σ error array is then

$$\sigma_f(i) = \sqrt{f(i)F_{\rm e}(i) + \sigma_{\rm d}^2(i)}, \tag{9}$$

where $\sigma_{\rm d}(i)$ is the noise contribution from the detector in each pixel. The S/N for each pixel can then be written as

$$\left(\frac{S}{N}\right)(i) = f(i)\sqrt{\frac{F_{\rm e}(i)}{f(i) + \beta_{\rm d}^2(i)}}, \tag{10}$$

where $\beta_{\rm d}(i) \equiv \sigma_{\rm d}(i)/\sqrt{F_{\rm e}(i)}$ is the ratio of the detector noise and photon noise expected from the envelope at pixel i. Assuming that $\sigma_{\rm d}(i) = \sigma_{\rm d}$ is constant for all pixels and recalling that $F_{\rm e}(i)$ varies slowly compared to $f(i)$, then the maximum S/N of the comb is

$$\left(\frac{S}{N}\right)_{\rm max} = \sqrt{\frac{F_{\rm e,max}}{1 + \beta_{\rm d,max}^2}}. \tag{11}$$

Therefore, in our simulations one specifies the S/N at all pixels by knowing the shape of the comb and envelope functions and by specifying the maximum signal-to-noise ratio, $({\rm S/N})_{\rm max}$, across the comb and a constant detector noise, $\sigma_{\rm d}$ or $\beta_{\rm d,max}$.

For our simulations, we assume that the envelope function is constant over the entire wavelength range of the comb. That is, all comb lines have equal intensity. The comb function can be modelled as a series of delta functions equally spaced in frequency according to the assumed laser repetition rate, $\nu_{\rm r}$. The delta functions are convolved with the spectrograph's IP which we assume to be a Gaussian of width specified by the resolving power R. For an echelle spectrograph R is roughly constant over the entire wavelength range and we make this additional assumption here. Simulated spectra are placed on a log-linear wavelength scale sampled at 3 pixels per resolution element (FWHM) in order to emulate one-dimensional reduced echelle spectra. A portion of simulated spectrum is shown in Fig. 3.

We calculate $\sigma_{\rm v}$ from the simulated spectra using equation (7). In calculating the derivative in equation (5), we have simply used the finite-difference derivative between successive pixels,

$$\frac{\partial F(i)}{\partial\lambda(i)} \approx \frac{F(i) - F(i-1)}{\lambda(i) - \lambda(i-1)}. \tag{12}$$

With this application, the first pixel of any spectral subdivision has undefined weight, $W(i)$. The sum in equation (7) therefore begins at the second pixel in each spectral subdivision.

An example of the results from the simulated comb spectra is shown in Fig. 4. Here, we assumed $R = 150\,000$ and $({\rm S/N})_{\rm max}$ of 500 per spectral pixel. Gemini/bHROS, ESO-3.6 m/HARPS and Subaru/HDS already operate at (or close to) this resolving power. To obtain $({\rm S/N})_{\rm max} = 500$ per pixel with modern CCDs, which typically have a linear response when fewer than ∼40 000 photoelectrons are detected per pixel, the comb spectrum would have to be spread over 6–7 pixels in the spatial direction; this is readily achievable with most modern echelle spectrographs. We also assumed a fairly typical wavelength range, 3800–8200 Å.

Fig. 4 demonstrates two important results. (i) The velocity precision available from each echelle order is ∼6−7 cm s^{-1} which

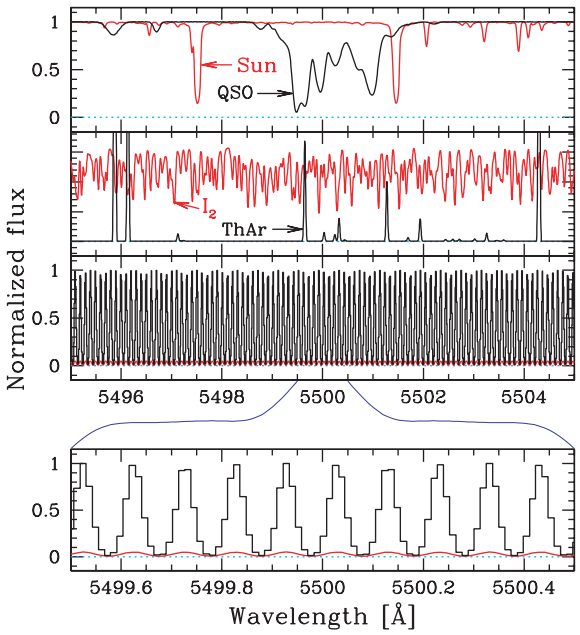

Figure 3. Comparison of small sections of simulated object spectra with different calibration spectra. The upper panel shows a model solar spectrum (red/grey line) and a low-ionization metal transition (arbitrary redshift) with typical velocity structure in a synthetic quasar absorption spectrum (black line). The next panel compares model spectra of an iodine absorption cell (red/grey line) and ThAr emission-line lamp (black line) at $R = 150\,000$ on different arbitrary flux scales. Note the complexity of the I_2 absorption spectrum and the relatively sparse distribution of ThAr lines with their large range of intensities. The third panel shows a simulated frequency comb echelle spectrum over the same wavelength region with repetition rate $\nu_r = 10$ GHz, resolving power $R = 150\,000$ and $(S/N)_{max} = 500$. The lower panel zooms in on a 1-Å wide section of the upper panel. For the comb spectra, the black histogram shows the expected flux while the red/grey solid line shows the error array exaggerated by a factor of 25.

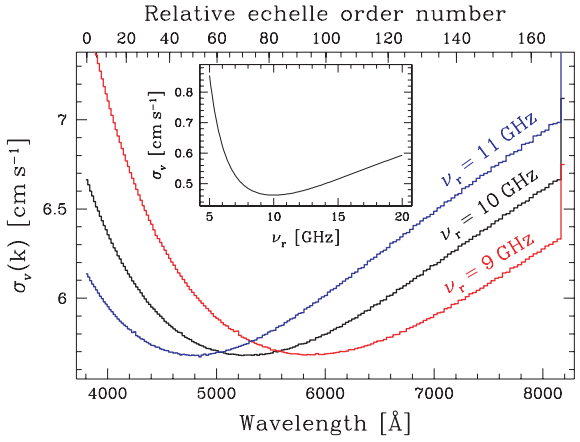

Figure 4. Results from comb simulations with $R = 150\,000$, $(S/N)_{max} = 500$ and $\beta_{d,max} = 0.01$. The spectrograph's resolution (FWHM) is sampled with 3 pixels and each echelle order is assumed to be 2048 pixels long. The main panel shows the expected velocity precision available from each echelle order, $\sigma_v(k)$, for three different line spacings while the inset shows the total velocity precision, σ_v, integrated over the full wavelength range of the simulated spectrum, 3800–8200 Å. For a comb spectrum of this resolution, the optimum line spacing (or repetition rate) is $\nu_r = 10$ GHz, resulting in a total velocity uncertainty of $\sigma_v = 0.45$ cm s^{-1}. σ_v rises sharply for repetition rates below the spectrograph's resolution (3.3 GHz at 6000 Å).

is consistent with the 'back-of-the-envelope' calculation in Section 3.1. This varies by $\lesssim$20 per cent across all echelle orders because the comb lines are uniformly separated in frequency space. (ii) The total velocity precision integrated over all echelle orders is 0.45 cm s^{-1} but, for a given R, this depends strongly on the comb line spacing. Assuming that each spectral resolution element is sampled at or above the Nyquist rate and the detector noise is small compared to the photon noise, the optimum line spacing required is determined by the resolving power:

$$\nu_r^{opt} \approx \frac{1.5 \times 10^6}{R}\ \mathrm{GHz} \sim 3\Delta\nu_{cent}, \qquad (13)$$

where $\Delta\nu_{cent}$ is the spectrograph's resolution in frequency space at approximately the centre of its wavelength range. Also, at constant R and $(S/N)_{max}$ (and again assuming $\beta_{d,max} \ll 1$), the increase in overall velocity uncertainty with increasing ν_r is simply described as $\sigma_v \propto \sqrt{\nu_r}$ provided that comb lines are well resolved from each other, i.e. $\nu_r \gtrsim 1.5\,\nu_r^{opt}$. The increase in σ_v with decreasing line spacing below ν_r^{opt} is extremely fast but has no simple analytic description. Suffice it to say that our simulations show that the increase is faster than exponential. Nevertheless, a total precision within a factor of 2 of the optimum can be achieved over the range $\nu_r \approx (0.5{-}5)\,\nu_r^{opt}$. Equivalently, a comb of fixed ν_r can be used to almost optimally calibrate spectra over a reasonable range in resolving power.

These results are easily scaled according to the parameters of different spectrographs. It is not surprising to find that $\sigma_v \propto 1/(S/N)_{max}$ and $\sigma_v \propto 1/R$ if, again, the sampling of each resolution element is adequate and $\beta_{d,max} \ll 1$. Thus, for a given resolving power and maximum S/N, the optimum photon-limited precision available over the wavelength range 3800–8200 Å is

$$\sigma_v^{opt} = 0.45 \left[\frac{500}{(S/N)_{max}}\right] \left(\frac{1.5 \times 10^5}{R}\right) \sqrt{\frac{\nu_r^{opt}}{10\ \mathrm{GHz}}}\ \mathrm{cm\,s^{-1}} \qquad (14)$$

$$= 0.45 \left[\frac{500}{(S/N)_{max}}\right] \left(\frac{1.5 \times 10^5}{R}\right)^{3/2}\ \mathrm{cm\,s^{-1}}. \qquad (15)$$

For example, with lower resolving powers typical of spectrographs like VLT/UVES and Keck/HIRES ($R = 70\,000$), and assuming that $(S/N)_{max} = 300$ can be easily obtained in a single comb exposure, a precision of $\sigma_v^{opt} = 2.4$ cm s^{-1} should be achievable. The pre-factor of 0.45 cm s^{-1} in equations (14) and (15) is larger for narrower wavelength ranges. For example, it is 0.63 cm s^{-1} for 4500–6500 Å.

3.4 Additional sources of error

The typical photon-limited precision of $\sim$1 cm s^{-1} calculated above is five orders of magnitude smaller than the typical pixel size for most modern echelle spectrographs. To provide some context, for a 15-μm pixel this corresponds approximately to the size of the silicon atoms making up the CCD substrate! Therefore, if the photon noise limit is to be reached, mitigation of possible systematic effects in the telescope, spectrograph and detector systems is imperative. Many such effects have already been considered for observations requiring short-term stability (approximately one night to approximately one week) which achieve 100-cm s^{-1} precision or better (e.g. Lovis et al. 2006). However, in pushing to the 1 cm s^{-1} precision level, additional sources of error will need to be considered in detail.

We will not conduct an exhaustive study of possible effects here but the following initial list is illustrative. (i) Inhomogeneities and variations in the intensity profile of the object and comb fibres presented at the spectrograph slit; (ii) variations in the spectrograph's

IP across the CCD; (iii) inaccuracies in the echelle grating's line markings; (iv) variations in pixel size and separation across an individual CCD array; (v) intra-pixel sensitivity variations and (vi) CCD temperature variations, especially during read-out. While pre-slit effects such as (i) clearly require their own solutions (in this case, efficient beam homogenization and stabilization), most post-slit effects such as (ii)–(vi) might be mitigated by using the frequency comb itself. Since the comb provides a series of closely spaced modes which are known, a priori, to have equidistant spacing, comb spectra could be used to accurately characterize the spectrograph and detector's response to different systematic effects. In practice, this would be facilitated by injecting the comb spectrum into the object fibre and by altering $\nu_{\rm r}$ and/or $\nu_{\rm ce}$ slightly to shift the comb spectrum by less than a resolution element. Thus, while the frequency comb would provide, in principle, a significant increase in precision, it would also provide an important means to characterize, measure and correct-for many systematic errors so that the available photon-limited precision could be realized in practice.

Aside from the spectrograph's IP, an additional factor contributing to asymmetries and variations in the measured point spread function could be intrinsic asymmetries in the comb modes themselves. Although the central frequencies of the modes are defined precisely by the self-referencing system, asymmetries in the modes' profiles could arise via correlated phase and amplitude noise, generally referred to as 'repetition-rate noise'. The time dependence (and therefore the time-averaging properties) of the asymmetry in individual modes will depend greatly on the type of laser comb system eventually employed. Nevertheless, since the spectral width of individual modes is typically $\sim$1 MHz (0.6 m s^{-1} at 6000 Å) and the asymmetry is expected to be small in comb systems stabilized to precise clocks, the difference between an individual mode's frequency and the centroid of its intrinsic profile should amount to no more than $\sim 1-10$ cm s^{-1}. If the asymmetries vary very slowly with time, this effect would be corrected for when modelling the overall point spread function. However, if mode profiles were found to vary on very short time-scales, additional techniques for reducing the mode line-width closer to the desired calibration uncertainty (i.e. $\sim$1 cm s^{-1} or 17 kHz at 6000 Å) might be employed (e.g. Diddams et al. 2003).

4 DESIGN CHALLENGES AND POSSIBLE SOLUTIONS

From the point of view of designing a real frequency comb calibration system, the most important result from the simulations in Section 3.3 is that laser repetition rates of $\nu_{\rm r} = 5-30$ GHz give the highest velocity precision for practical spectrograph resolving powers of $R = 50\,000-300\,000$ (equation 13). Although high repetition rate (>10 GHz) lasers with picosecond pulses and frequency combs with broad spectral coverage, sub-100 fs pulses and low repetition rate (<1 GHz) have been demonstrated, the desired combination of high repetition rates, short pulses and large spectral widths (e.g. $\sim$3800–8200 Å) is challenging and is yet to be experimentally demonstrated. A uniform intensity distribution across the whole wavelength range is also highly desirable since this ensures that similar velocity precision can be obtained from any spectral sub-division. Below, we discuss why these design requirements may be problematic and offer some possible solutions.

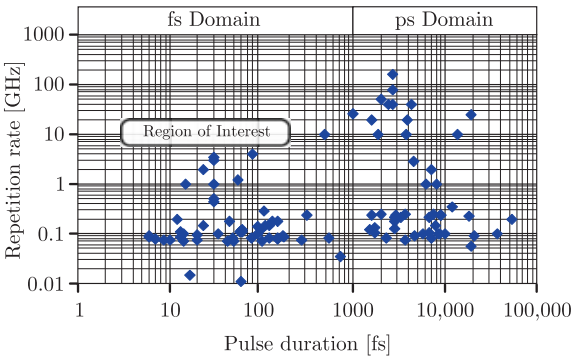

Figure 5. A review of femtosecond laser performance data shows two distinct clusters, one in the 10–200 fs regime and the other in the 1–20 ps regime of pulse durations. Sub-100 fs pulse lasers seem to operate to up to 4 GHz. The region of interest (5–30 GHz repetition rate, 3–200 fs pulse duration) is still new territory for femtosecond pulsed lasers.

4.1 Repetition rate

Reaching the optimum repetition rate suggested by Fig. 4 is not, by itself, challenging; several systems with even higher $\nu_{\rm r}$ already exist. For example, Lecomte et al. (2005) published a mode-locked laser with $\nu_{\rm r} = 40$ GHz. Unfortunately, the peak power of such lasers is so low that they cannot use the fast but weak pulse shaping and shortening mechanisms that are usually provided by the Kerr effect. Instead, these lasers rely on slow saturable absorbers for mode locking, forcing pulse durations into the picosecond regime with the associated narrow spectral widths. Indeed, the spectral width would need to be $\gtrsim$30 times larger to maintain the comb's coherence in the spectral broadening process discussed in Section 4.2. The challenge of generating sub-100 fs pulses at repetition rates $\gtrsim$10 GHz is illustrated by a review of the performance of ultrafast lasers in the literature, as summarized in Fig. 5. To our knowledge, the highest repetition rate achieved so far in the sub-100 fs regime is $\nu_{\rm r} \approx 4$ GHz (Leburn et al. 2004).

One possible way to combine high repetition rate, short pulses and large spectral width is to spectrally filter the laser beam outside the cavity. The strategy would be to use a laser with modest repetition rate, say $\nu_{\rm r} \sim 2$ GHz, where reasonably short pulses can still be generated and where there is still enough energy per pulse to allow efficient spectral broadening (as discussed in Section 4.2). The effective mode spacing could then be increased by filtering out most modes with a Fabry-Perot etalon with a free spectral range (FSR) chosen to be an integer multiple of $\nu_{\rm r}$ and equal to the final desired mode spacing (e.g. Udem et al. 1999). The etalon would be required to have highly stable transmission fringes and a high enough finesse to ensure strong suppression of the extraneous modes.

Fig. 6 shows an etalon transmission function defined by the FSR, mode suppression ratio in decibels ($\rho_{\rm dB}$), and by a repetition rate enhancement factor $q \equiv {\rm FSR}/\nu_{\rm r}$. Since the cavity transmission profile should be adequately described by an Airy function, the required finesse of the etalon cavity is uniquely determined by $\rho_{\rm dB}$ and q:

$$F = \frac{\pi}{2}\frac{\sqrt{10^{\rho_{\rm dB}/10}-1}}{\sin(\pi/q)} \approx \frac{q}{2}10^{\rho_{\rm dB}/20}, \qquad (16)$$

where the approximation is accurate for suppression ratios >10 dB and $q \gg 1$. For example, the approximation is correct within 1.6 per cent for $\rho_{\rm dB} = 50$ dB and $q = 10$. For a 10-GHz FSR, a side-mode suppression of $\rho_{\rm dB} = 50$ dB can be achieved by eliminating three

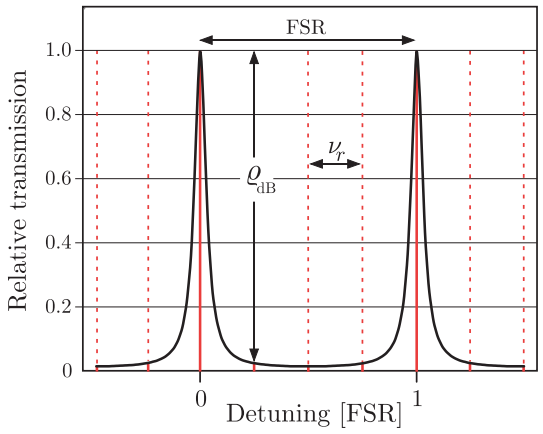

Figure 6. Simple representation of the (Fabry-Perot) transmission profile of an idealized mode-filter cavity (black curves). The resulting mode spacing is given by the FSR between transmission peaks. The degree to which the intervening modes are suppressed is specified by the side-mode suppression ratio, $\rho_{\rm dB}$, measured at the position of the strongest off-resonant mode. Achieving strong side-mode suppression requires a high finesse according to equation (16).

out of every four modes (i.e. $q = 4$) from a $\nu_{\rm r} \sim 2.5$ GHz comb, requiring a finesse of $F \approx 700$. Such a repetition rate and finesse are achievable with current technology and so this mode-filter technique seems a promising approach to achieve higher effective repetition rates. However, one challenge will be for a large spectral range to be filtered in this way because the dispersion of the cavity components will create differing path lengths in light of widely different wavelengths. The etalon mode spacing remains constant only if the dispersion is compensated properly. Simultaneously achieving reliable dispersion compensation and high finesse/reflectivity may impose a challenge for the etalon mirror design (Gohle et al. 2005). A practical solution might employ several frequency combs and etalons which each covers a narrower spectral range.

4.2 Spectral width

In most octave-spanning frequency combs, the process of self-phase modulation is used to extend the comb's spectral width. For example, titanium–sapphire femtosecond laser pulses launched into photonic crystal fibres or micro-structured fibres have shown extensive spectral broadening and this has been used for generating frequency combs with $\nu_{\rm r}$ up to 1 GHz (e.g. Holzwarth et al. 2000; Jones et al. 2000). In this process, the spectral coverage is increased fairly symmetrically around the central wavelength of the pulses and a total spectral coverage from 4500 Å to 1.4 μm has been achieved. Similarly, lasers based on Er-doped fibres emitting around 1.5 μm have produced spectra covering 5000 Å to 2.2 μm at $\nu_{\rm r}$ up to 250 MHz (e.g. Nicholson et al. 2003; Mackowiak et al. 2005).

However, producing broad spectra at higher repetition rates is difficult because the self-phase modulation process requires a certain pulse peak power to provide an octave of broadening. Assuming a pulse train at $\nu_{\rm r}$ with an average power, $\langle P \rangle$, the peak power is roughly given by the energy in one pulse, $\langle P \rangle / \nu_{\rm r}$, divided by the pulse duration. Typically, a pulse energy of 2 nJ for 100-fs pulses is needed, translating to average powers of 2 & 20 W for 1 & 10 GHz repetition rates, respectively. In practice, $\langle P \rangle$ in mode-locked lasers have so far been limited to ∼1 W. Thus, the highest repetition rates achieved so far for octave-spanning combs are around $\nu_{\rm r} \sim 1$ GHz. The fact that sufficient self-phase modulation requires a certain pulse peak power means that, in practice, broad spectra can be produced only with relatively low $\nu_{\rm r}$ while achieving higher $\nu_{\rm r}$ reduces the peak pulse power below that required for sufficient broadening. For example, the repetition rate of 4 GHz demonstrated by Leburn et al. (2004) is already close to optimal for very high spectrograph resolutions $R \sim 300\,000$ (equation 13). With a modest effort to filter the modes with an etalon, the effective repetition rate could probably be increased to $\gtrsim$10 GHz. However, this laser emits between 1.40 and 1.58 μm, so significant non-linear conversion processes would be required, such as frequency doubling (or tripling), or spectral shifting and broadening; the pulse peak power is too low at such high repetition rates for these processes to be effective.

On the other hand, a new class of mode-locked lasers, optimised for larger spectral width rather than shorter pulses, is currently under development. Such systems have reached spectral widths extending from 5700 Å to 1.3 μm (Mücke et al. 2005) at repetition rates up to 1 GHz. However, even these broad spectra are not yet sufficient to cover the entire optical region, especially the blue region of the spectrum. The current limitation is actually due to the laser cavity mirrors which do not operate efficiently outside this (already relatively broad) range.

Another option to achieve the desired effective spectral width could be the use of very fast and efficient optical phase modulators. These so-called 'optical frequency comb generators' (e.g. Kourogi, Nakagawa & Otshu 1993; Imai, Kourogi & Otshu 1998) are capable of adding several hundred modulation side bands to the spectrum of a single-mode laser with separations at the required optimal mode spacing (i.e. ∼10 GHz). However, so far the spectral width of these comb generators is insufficient for covering the whole optical range. Therefore, dozens (even hundreds) of generators would have to be used simultaneously or some advanced scanning method would have to be devised which allowed the full calibration region to be swept with a single generator (or perhaps many) within the exposure time.

In summary, designing a frequency comb covering the entire optical range while maintaining a high repetition rate would require some improvements in comb technology. A practical solution might employ a combination of mode filtering stages and non-linear conversion stages, possibly with additional amplifier stages to keep the power sufficiently high.

4.3 Uniform intensity

Unlike the sketch in Fig. 1, real frequency combs display strong intensity structure; intensity variations of two orders of magnitude are to be expected, even over relatively short wavelength ranges (∼300 Å), especially when using photonic crystal fibres for spectral broadening (e.g. Holzwarth et al. 2001). The intensity structure is also sensitive to the polarization and peak power of the pulses coupled into the non-linear fibre. They therefore vary with time as the laser–fibre coupling and laser parameters change. Fortunately, since only a small amount of power is required to fully expose the CCD (amounting to ∼40 000 photons per CCD pixel over ∼10–3600 s exposure times), the spectrum can be flattened by an attenuation mechanism which can respond to both spectral and time variations. One such mechanism, for example, might be a spatial light modulator (e.g. Weiner 2000) whereby groups of modes (i.e. small chunks of the comb spectrum) can be separated, differentially attenuated and recombined again. An alternative approach is to

improve the matching of phase velocities ('phase matching') between the various modes in the non-linear broadening process. This can be achieved by tailoring the longitudinal dispersion properties of the fibre and has been shown both theoretically and experimentally to produce broad, flat spectra (Hori et al. 2004).

5 CONCLUSION

We have outlined the possible use of frequency combs as calibration sources in astronomical echelle spectroscopy. Such combs generate a series of equally spaced, very narrow modes which, by employing self-referencing (or possibly other calibration) techniques, have absolute frequencies which are known a priori to relative precisions better than 10^{-12}. These are significant advantages compared to the properties of other calibration sources such as ThAr emission-line lamps and I_2 absorption cells. Simulations of comb spectra with uniform intensity over the optical range were sampled according to the properties of typical high-resolution echelle spectrographs and CCD detectors. These revealed that the laser repetition rate must be $\nu_r \sim 10-20$ GHz to produce optimal line spacings for $R \sim 50\,000 - 200\,000$ spectrographs. For such systems, the photon-limited wavelength calibration precision is in the cm s^{-1} regime when integrated over $\sim$1000 Å ranges and is generally $\lesssim$10 cm s^{-1} when integrated over individual echelle orders. The regular grid of comb lines would also greatly facilitate the tracking and effective removal of systematic distortions of the wavelength scale which might be produced through a variety of different effects in the telescope, spectrograph and detector systems. The absolute wavelength calibration would therefore be stable over very long time-scales even if elements of the spectrograph or comb changed. Indeed, frequency comb calibration would place spectra observed on different telescopes at different times on the same absolute, high-precision wavelength scale.

However, the results of the simulations reveal several challenges in designing and implementing a working comb calibration system. First, stable self-referenced combs with repetition rates of $\nu_r \sim 10-20$ GHz and which cover the entire optical range have not yet been realized. Another significant challenge will be to ensure that the comb envelope function – the peak intensity of the comb lines – is uniform over the wavelength range of interest. Nevertheless, the frequency comb technology is improving at a rapid pace and we expect that these challenges might be overcome by a relatively small research and development effort. The potential gain is clear: frequency comb calibration may effectively remove wavelength calibration uncertainties from all practical high-resolution spectroscopy and may allow the reliable combination of data taken on different telescopes over many decades.

ACKNOWLEDGMENTS

We are indebted to Savely Karshenboim for first suggesting the possibility of using frequency combs for wavelength calibration of astronomical spectra and to Robert Wynands for many early discussions about the practicality of such a system. We thank Victor Flambaum and Jochen Liske for many informative and helpful discussions. MTM thanks STFC for an Advanced Fellowship at the IoA.

REFERENCES

Bahcall J. N., Sargent W. L. W., Schmidt M., 1967, ApJ, 149, L11
Baranne A. et al., 1996, A&AS, 119, 373
Bauch A., 2003, Meas. Sci. Technol., 14, 1159
Bouchy F., Pepe F., Queloz D., 2001, A&A, 374, 733
Brault J. W., 1987, Mikrochimica Acta, 3, 215
Diddams S. A., Bartels A., Ramond T. M., Oates C. W., Bize S., Curtis E. A., Bergquist J. C., Hollberg L., 2003, IEEE J. Selected Topics Quantum Electron., 9, 1072
Fortier T. M., Bartels A., Diddams S. A., 2006, Opt. Lett., 31, 1011
Gohle C., Udem Th., Herrmann M., Rauschenberger J., Holzwarth R., Schuessler H. A., Krausz F., Hänsch T. W., 2005, Nat, 436, 234
Grazian A. et al., 2007, A&A, submitted
Holzwarth R., Udem Th., Hänsch T. W., Knight J. C., Wadsworth W. J., Russell P. S. J., 2000, Phys. Rev. Lett., 85, 2264
Holzwarth R., Reichert J., Udem Th., Hänsch T. W., 2001, Laser Phys., 11, 1100
Hori T., Takayanagi J., Nishizawa N., Goto T., 2004, Opt. Express, 12, 317
Imai K., Kourogi M., Otshu M., 1998, IEEE J. Quantum Electron., 34, 54
Ivanchik A., Petitjean P., Varshalovich D., Aracil B., Srianand R., Chand H., Ledoux C., Boissé P., 2005, A&A, 440, 45
Jones D. J., Diddams S. A., Ranka J. K., Stentz A., Windeler R. S., Hall J. L., Cundiff S. T., 2000, Sci, 288, 635
Knight J. C., Birks T. A., Russell P. S. J., Atkin D. M., 1996, Opt. Lett., 21, 1547
Kourogi M., Nakagawa K., Otshu M., 1993, IEEE J. Quantum Electron., 29, 2693
Leburn C. G., Lagatsky A. A., Brown C. T. A., Sibbett W., 2004, Electron. Lett., 40, 805
Lecomte S. et al., 2005, IEEE J. Quantum Electron., 41, 45
Loeb A., 1998, ApJ, 499, L111
Lovis C. et al., 2006, Nat, 441, 305
Mackowiak V., Kubina F., Adel P., Hänsch T., Holzwarth R., 2005, in Quantum Electron. Laser Sci. Conf. Vol. 2, QELS'05. Opt. Soc. America, Washington, DC, p. 1188
Marcy G. W., Butler R. P., 1992, PASP, 104, 270
Marcy G. W., Butler R. P., 1996, ApJ, 464, L147
Matos L., Kleppner D., Kuzucu O., Schibli T. R., Kim J., Ippen E. P., Kaertner F. X., 2004, Opt. Lett., 29, 1683
Mayor M., Queloz D., 1995, Nat, 378, 355
Mayor M. et al., 2003, The Messenger, 114, 20
Mücke O. D., Ell R., Winter A., Kim J.-W., Birge J. R., Matos L., Kärtner F. X., 2005, Optics Express, 13, 5163
Murphy M. T., Webb J. K., Flambaum V. V., Dzuba V. A., Churchill C. W., Prochaska J. X., Barrow J. D., Wolfe A. M., 2001, MNRAS, 327, 1208
Murphy M. T., Webb J. K., Flambaum V. V., 2003, MNRAS, 345, 609
Murphy M. T., Flambaum V. V., Webb J. K., Dzuba V. V., Prochaska J. X., Wolfe A. M., 2004, Lecture Notes Phys., 648, 131
Nicholson J. W. et al., 2003, Opt. Lett., 28, 643
Pasquini L. et al., 2006, in Whitelock P., Dennefeld M., Leibundgut B., eds, IAU Symp. Ser. Vol. 232, Scientific Requirements for Extremely Large Telescopes. Cambridge Univ. Press, Cambridge, p. 193
Reichert J., Holzwarth R., Udem Th., Hänsch T. W., 1999, Opt. Commun., 172, 59
Reinhold E., Buning R., Hollenstein U., Ivanchik A., Petitjean P., Ubachs W., 2006, Phys. Rev. Lett., 96, 151101
Rupprecht G. et al. 2004, in Moorwood A. F. M., Iye M., eds, Proc. SPIE Vol. 5492, Ground-based Instrumentation for Astronomy. SPIE, Bellingham, p. 148
Sandage A., 1962, ApJ, 136, 319
Udem Th., Reichert J., Holzwarth R., Hänsch T. W., 1999, Phys. Rev. Lett., 82, 3568
Udem Th., Holzwarth R., Hänsch T. W., 2002, Nat, 416, 233
Varshalovich D. A., Levshakov S. A., 1993, J. Exp. Theor. Phys. Lett., 58, 237
Webb J. K., Flambaum V. V., Churchill C. W., Drinkwater M. J., Barrow J. D., 1999, Phys. Rev. Lett., 82, 884
Weiner A. M., 2000, Rev. Sci. Instrum., 71, 1929
Ye J., Ma L. S., Hall J. L., 2001, Phys. Rev. Lett., 87, 270801

This paper has been typeset from a TEX/LATEX file prepared by the author.